nature geoscience

SUPPLEMENTARY INFORMATION

DOI: 10.1038/NGEO752

This section includes additional information for the model parameters as well as the results of a set of sensitivity experiments to illustrate the dependence of the model behavior on different parameter values than those used in the standard simulation (discussed in the main text):

SOM #1 gives additional information about model parameters.

SOM #2 illustrates the sensitivity of the model to initial conditions.

SOM #3 presents the results of sensitivity tests to the external forcing signal.

SOM #4 illustrates the dependence on different postulated D-O cycle periodicities.

SOM #5 corresponds to a detailed set of sensitivity experiments to the *Lc* parameter (i.e. critical length value of the ice shelf to change the ice flow mode).

SOM #6 considers the impact of different calving laws.

SOM #7 presents some conclusions of the Supplementary Online Material

SOM #1: Model parameters

The k_{stream} and k_d values have been deduced from the basal dragging coefficients used in the 3D ice sheet model GRISLI to properly simulate the Antarctic ice velocities[31]. The maximum ice stream velocity (k_{stream} = 5 m/yr in the model, and 5000 m/yr when accounting for the aspect ratio) is allowed when the buttressing effect is minimum.

k_{bm}, bm_0 have been adjusted to ensure the global mass conservation in the standard simulation. With the chosen values of k_{bm} and bm_0, the basal melting rate under the ice shelf ranges between 0.825 (melting) and -0.325 m/yr (negative values indicate ice accretion). These values have been deduced from remote sensing observations[32].

Through a set of sensitivity tests, three parameters (L_c, H^2_{calv}, and k_{calv}) have been revealed to be crucial for the model behavior and are discussed in the following sections presenting systematic sensitivity studies to these parameters.

Conceptual models are certainly useful to propose a new physical framework and new processes that may explain climate variability[33]. To obtain accurate quantitative issues, these processes have to be implemented in more sophisticated climate-cryosphere models.

DOI: 10.1038/NGEO752

Nevertheless, our model produces freshwater and iceberg fluxes (0.05–0.25 Sv) that are fully consistent with both the simulated effects on the glacial ocean derived from a sophisticated atmosphere-iceberg-ocean model[34] and with the $\delta^{18}O$ excursions observed during Heinrich events[35].

SOM #2: Initial conditions

As mentioned in the main text, when the system is forced by a constant basal melting rate, the model does not reproduce any oscillation and rapidly tends towards the equilibrium.

However, the question which arises is whether this behavior is still observed when the initial conditions are pushed away from those of the standard simulation (H_1 = 3000 m and H_2 = 400 m) or those simulated in the standard run resulting from the mechanism we propose here (H_1 between 2600 and 3200 m and H_2 between 200 and 1000 m). In other words: Is there a hidden periodical solution of the system only accessible for specific initial conditions when the system is forced by a constant basal melting rate?

To answer this question we carried out two additional experiments. In the first one (Fig. S1a), the initial conditions (H_1 = 4000 m and H_2 = 200) correspond to a large grounded ice sheet and to a thin ice shelf, whereas in the second test, a small ice sheet and a thick ice shelf have been considered ($H_1 = H_2$ = 1000 m). Although these two sets of values are not fully realistic, these experiments are designed to test the model behavior to conditions that are not spontaneously reached by the system.

In the first case, the non-buttressed mode is instantaneously reached. This leads to a major surge which removes ice from the grounded part, thereby feeding the floating part. The shelf then gains mass until its length becomes greater than L_c and the buttressed mode is recovered. Subsequently, ice velocities fall down, the shelf is no longer perturbed by ice advection from the grounded part and the model asymptotically tends towards the equilibrium.

In the second experiment, the non-buttressed mode cannot be reached because there is no process allowing the acceleration of the ice flow at the grounding line. The growth of the grounded ice sheet is mainly driven by the snow accumulation. The shelf loses mass through basal melting because it is poorly fed by the grounded part. The model then tends to the equilibrium without exhibiting any oscillation.

These experiments show that the mass exchange between the grounded ice sheet and the ice

shelf is not sufficient to generate oscillations. Therefore, the periodical behavior of the model in the standard simulation does not result from any hidden periodical solution of the ice flow system. To put the system into an oscillatory behavior, it is necessary to consider an external forcing acting on the ice-shelf length.

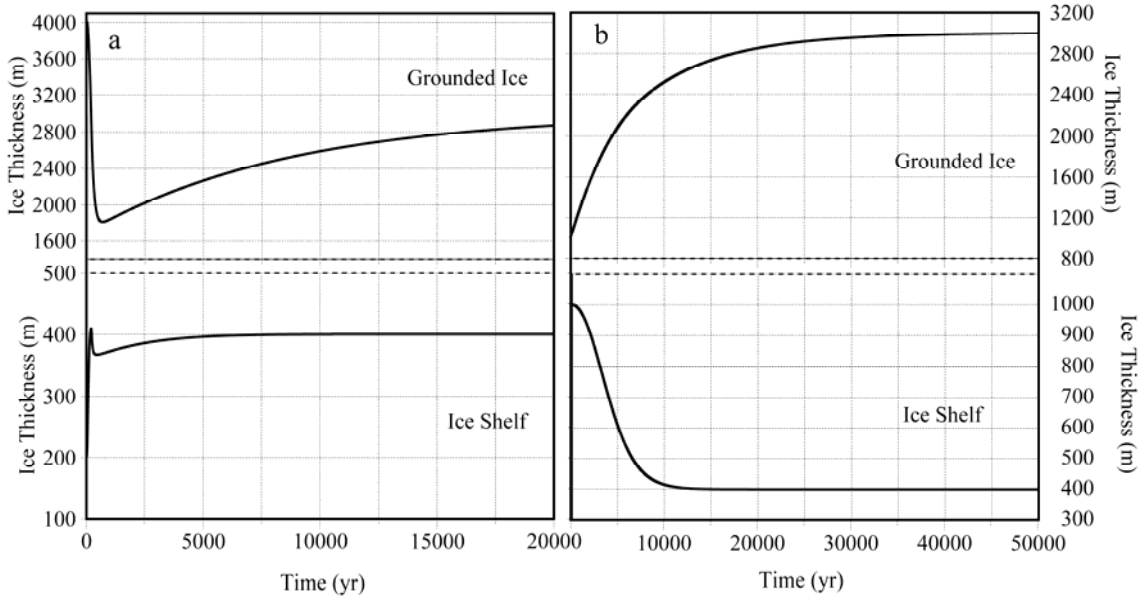

Figure S1.Test to the initial conditions under constant forcing.

Temporal evolution of the grounded and ice-shelf thickness. H_1=4000 m., H_2=200 m. (a) and H_1=1000 m., H_2=1000 m. (b) where H_1 and H_2 respectively correspond to the grounded ice and the ice-shelf thickness.

SOM #3 Dependence on the external forcing signal

The previously announced external forcing has been considered in the main text as periodical variations of the basal melting rate. This is justified by the fact that during glacial periods, the oceanic temperatures under the ice shelves were likely to be subjected to drastic changes due to different modes of ocean circulation that accompanied the shift from stadial to interstadial climate conditions. However, other processes such as the interannual climate variability or changes in regional oceanic circulation under the ice shelves may have also induced variations of the basal melting rate. Nevertheless, at the millennial time scale these processes can be considered to act as noise.

DOI: 10.1038/NGEO752

To test the impact of these processes, we built up a new external forcing signal only composed of a white noise (equal spectral density for all frequencies). We carried out experiments for two different amplitudes of this noise (4.95 and 12.375 m/yr), respectively 4 and 11 times greater than the amplitude of the standard periodical forcing. In addition, we performed two other experiments in which the periodic forcing used in the standard simulation has been superimposed to these noise signals. The model dependence to these external forcings is illustrated in figures S2 and S3. Figure S2 shows the evolution of the grounded ice thickness for these four simulations and Figure S3 displays the "waiting time" interval distribution of the ice surges.

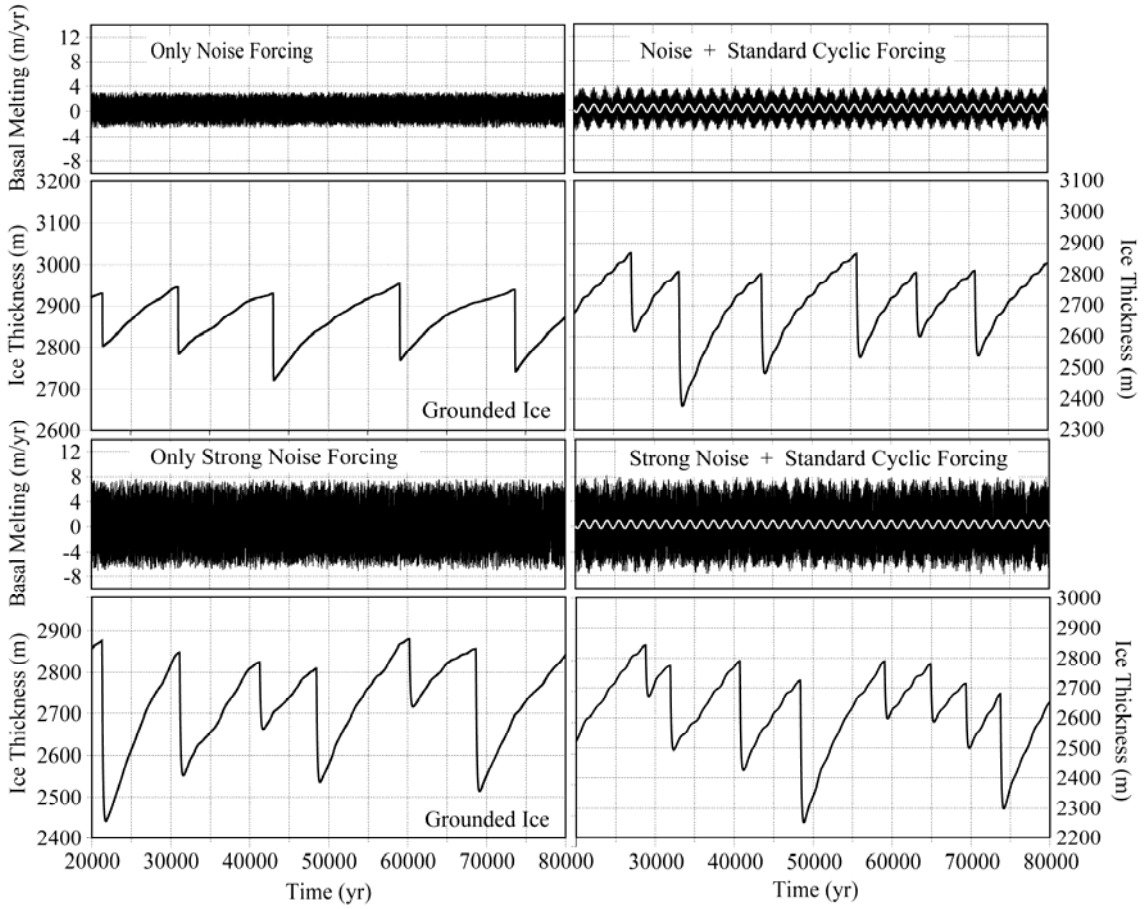

Figure S2. Sensitivity tests to different noises. Temporal evolutions of the basal melting (oceanic forcing) and of the grounded ice thickness. The noise amplitudes are respectively 4.95 and 12.375 m/yr, while the standard sinusoidal forcing presents an amplitude of 1.15 m/yr. The highest amplitude noise is referred as "strong noise", and the smallest one is simply referred as "noise".

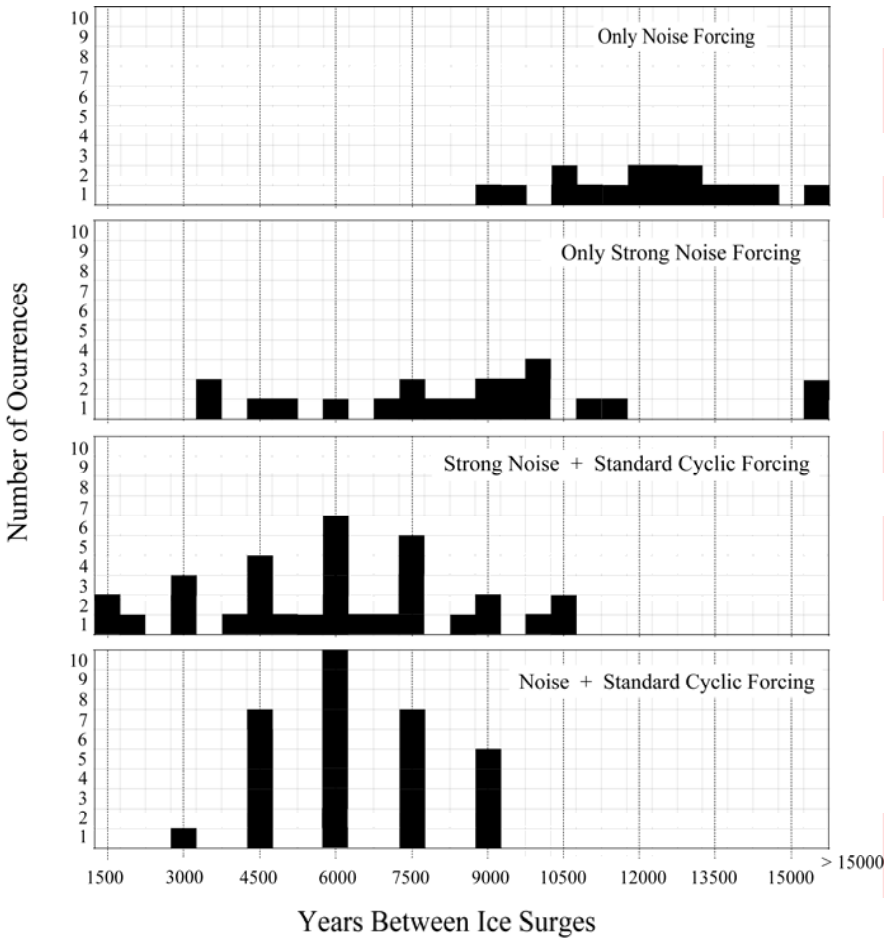

Figure S3. Interspike interval distribution.

The waiting time between two consecutive ice surges is counted for each of the four simulations defined in figure S2. Each distribution was obtained from a simulation of 200 000 model years. (the first 80 000 years are shown in figure S2).

"Only Noise Forcing" experiment: Forcing the model with only a noise signal is sufficient to reproduce an oscillatory behavior. In this simulation, the simulated periodicities are randomly distributed (no privileged intervals of periodicities) between ~ 9000 and 15000 years: here the model presents a slow reactivity because the waiting time between two oscillations is at least ~ 9000 years.

"Only Strong Noise Forcing" experiment: When the forcing is given by the highest amplitude noise signal, the model still behaves randomly, but the waiting time between ice surges is decreased. This indicates a greater reactivity of the system. This result was expected because the probability for the ice shelf to reach the threshold length L_c is enhanced with a noise of larger amplitude. This favors the non-buttressed mode and therefore the ice surge.

"Strong Noise + Standard Cyclic Forcing" experiment: If the standard periodical forcing

DOI: 10.1038/NGEO752

signal is superimposed to the strongest noise, a relative discretization of the interspike distribution appears. Periodicities appearing as multiples of those of the standard oceanic forcing are more frequent.

"Noise + Standard Cyclic Forcing" experiment: When the periodical oceanic forcing is superimposed to the smallest amplitude noise, all the ice surges occur at periodicities that are exactly some multiples of the standard oceanic forcing period. From this point of view, this latter experiment gives results close to those obtained in the standard simulation, with a pronounced peak distribution for the 6000 yr period.

SOM #4: Dependence on the forcing period: D-O cycle

In climate records, the D-O cycle periodicity is not constant as considered in the standard simulation (1.5 kyr). Other studies[22] suggest a range between 1.5 and 6 kyr between two consecutive D-O events. Accordingly, the model has been tested under different forcing signals with periodicities ranging from 1500 (standard simulation) to 6000 years.

A spectral analysis of the resulting ice velocities (Figure S4) still reveals the occurrence of resonant periodicities. For τ =6,000 yr the forcing period coincides with the greatest peak of the model spectrum (ice streams and ocean oscillates in phase).

In all other cases the major model response arises as a resonance phenomenon. This indicates that, when the forcing signal is composed of the superimposition of different periodic signals, the model is still able to produce ice flow oscillations with periodicities larger than that of the standard forcing. Moreover, these simulated periodicities remain consistent with those deduced from climatic archives.

Note that the ice velocities reproduced in these experiments range from 1 to 5 m/yr (1000 to 5000 m/yr, when considering the model aspect ratio) in the non-buttressed mode, and from 0.1 to 0.3 m/yr for the buttressed mode (100 to 300 m/yr, when considering the model aspect ratio). These values are fully consistent with both the sliding velocities in the binge-purge based ice surges[5] and with the Antarctic ice streams velocities[7,31].

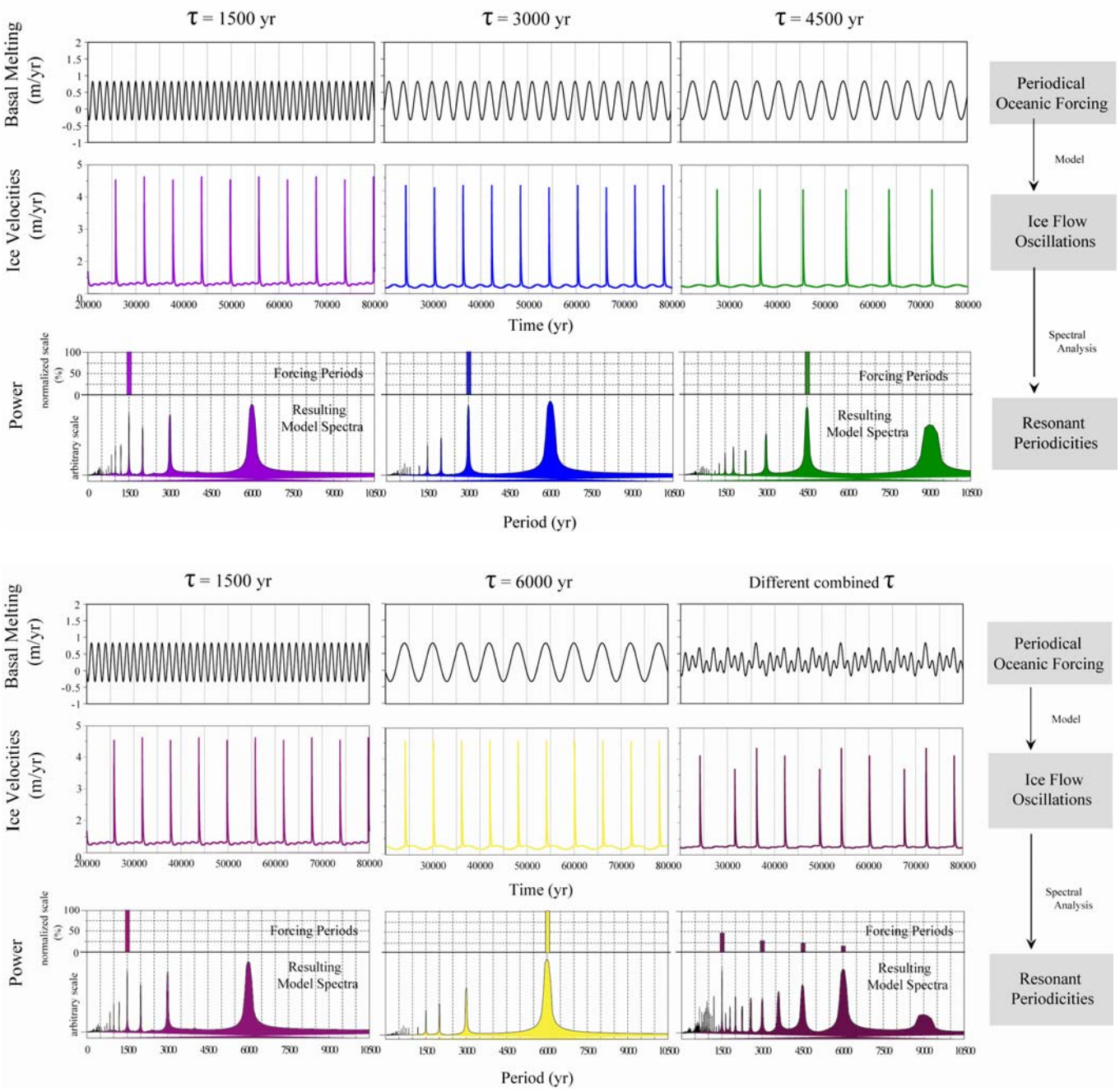

Figure S4. Sensitivity tests to different oceanic forcing periods.

τ=3,000 yr., τ=4,500 yr., τ=6,000 yr., and different combined τ, following the equation:

$$Bm(t) = k_{bm}\left(0.4\times\cos\left(\frac{2\pi}{\tau_1}t\right)+0.3\times\cos\left(\frac{2\pi}{\tau_2}t\right)+0.2\times\cos\left(\frac{2\pi}{\tau_3}t\right)+0.1\times\cos\left(\frac{2\pi}{\tau_4}t\right)\right)+Bm_0$$

Temporal evolution of the basal melting (oceanic forcing) and ice velocities at the grounding line, and spectral analysis (Fast Fourier transform) of each one of the five different simulations.

DOI: 10.1038/NGEO752

SOM #5: Dependence on the ice-shelf length threshold for the ice flow

A set of sensitivity tests has been performed by considering a large range of L_c values. Results are illustrated in figure S5 and show a high dependency of the model periodicities on this parameter.

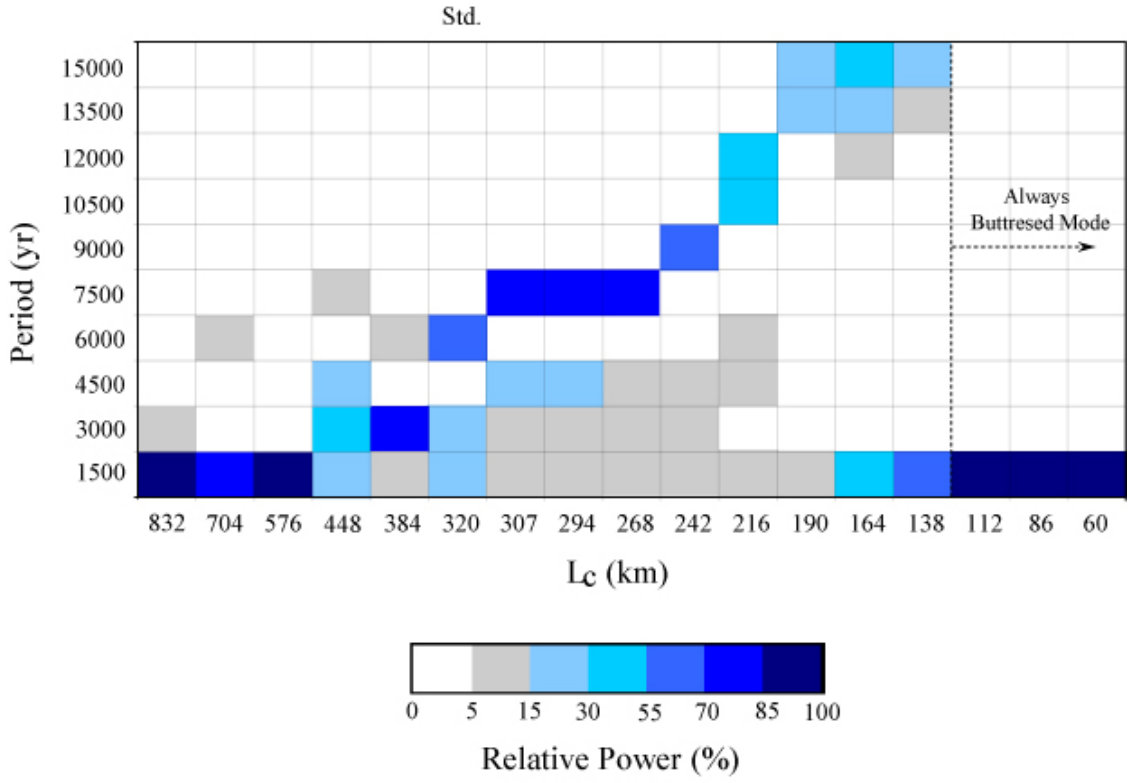

Figure S5. Sensitivity tests to the L_c parameter.

Different values of this parameter are considered in the horizontal axe. For each one of these values a model simulation of 200000 climate years has been carried out. The resulting periodicities of a spectral analysis of each simulation are represented in the vertical axe. Colours illustrate the relative magnitude (in %) of these periodicities.

For high L_c values (>500 km) oscillations are generated in a 1500 yr period. The ice-shelf length can easily shrink below these high *Lc* values and in that case the non-buttressed mode is activated (and an ice surge occurs) for each oceanic cycle.

For a L_c value < 500 km ice surges occur less frequently and a resonance appears for the 3000, 4500 and 6000 yr periods.

For lower L_c values, the simulated periodicities increase because the probability to fulfill the condition $L < Lc$ (shift into the non-buttressed mode) becomes progressively lower. The model periodicity may reach a maximum of 15000 yr (10 times the oceanic forcing, τ) for

Lc~130 km. If L_c becomes lower than 110 km, the system falls into a new mode: The $L<L_c$ condition is never fulfilled and the model remains always in the buttressed mode; in that case no ice surge can be produced and the ice velocities are only slightly modulated by the ice-shelf length variations driven by the basal melting forcing.

Figure S5 clearly shows that the ice flow oscillations required to produce HEs in our model occur for a large area of the L_c parameter phase space. This aspect further contributes to reinforce the robustness of the HEs mechanism that we propose here.

SOM #6: Calving

Modeling calving is a difficult task and, even in comprehensive 3D ice sheet models, this process is often not explicitly simulated. In a recent paper, Alley[28] proposed an empirical calving law based on Antarctic ice shelf observations. However, the calving equation considered in this work is significantly different. The goal of this section is to justify our formulation and assess the sensitivity of our model to this process.

The calving law described in the main text and used in the standard simulation is a threshold-based equation that can be considered as a specific case of a more general calving law:

$$Calv(t) = k_{calv}(t) H_2(t)$$

Where:

$$k_{calv} = k^1_{calv} + k^2_{calv} + k^3_{calv}$$

k^1_{calv} is constant and represents the minimum calving rate. k^2_{calv} introduces a threshold on ice shelf thickness (inactive for thick iceshelves):

$$k^2_{calv}(t) = k^2_{calv} \quad if \quad H_2(t) < H_2^{Calv}$$

$$k^2_{calv}(t) = 0 \quad otherwise$$

As mentioned in the main text, when the ice shelf is thin, the ratio between crevasses depth and ice thickness is high; this may weaken the ice shelf and lead to high calving rate. This process does not appear in Alley's empirical law. This law is based on a steady-state hypothesis and could not be applied for highly non-linear cases as in ice shelf disintegration.

k^3_{calv} introduces a threshold on spreading.

$$k^3_{calv}(t) = k^3_{calv} \quad if \quad Non\text{-}Buttressed\ Mode$$

DOI: 10.1038/NGEO752

$$k_3(t) = 0 \quad otherwise$$

If the conditions k^1_{calv} =0 and $k^2_{calv} = k^3_{calv}$ are fulfilled, the calving law equation we used in the main text arises.

Figure S6a illustrates the most general case of k^1_{calv} =$k^2_{calv} = k^3_{calv}$, where a permanent calving rate dependent on the ice-shelf thickness has been added. Major calving episodes (HEs) can still be identified when the non-buttressed mode conditions are reached. The effect of changing the *Lc* threshold has been largely discussed in the previous section.

The H_2^{Calv} parameter determines the amplitude and the duration of the minor calving episodes. However, changing the H_2^{Calv} parameter value does not have any impact for the model behaviour.

To assess the realism of the calving rates used in this study, we performed a set of sensitivity experiments (similar to that shown in SOM #5) on the k_{calv} parameter. A resonant condition (ie. HEs-like flux oscillations) has been found for the range:

$$0.125 \times 10^{-3} < k_{calv} < 12.5 \times 10^{-3} \text{ (yr}^{-1}\text{)}$$

Considering a mean ice-shelf thickness of 500 m, and re-scaling according to the aspect model ratio, k_L, this resonant condition can be expressed as:

$$62.5 < CalvingRate < 6250 \text{ (m/yr)}$$

In other words, our model is able to reproduce the oscillatory behavior described in the main text as long as the resulting mean calving values are comprised within that range. These values are fully consistent with those recently measured in Antarctic ice shelves. Any change in the k_{calv} value within this range only slightly modulates the periodicities shown in the standard simulation. This confirms that the key parameter for the model falling into an oscillatory behavior is L_c.

Therefore, ice flux oscillations can be generated for a large range of H_2^{Calv} and k_{calv} values. Nevertheless, to qualitatively conciliate ice flux oscillations with major calving episodes (i.e. HEs-like iceberg discharges) another additional condition is required:

$$k^1_{calv} \leq k^2_{calv} \leq k^3_{calv}$$

Otherwise, the major peaks of iceberg discharge could occur out of phase with the enhanced ice velocities at the grounded line.

Finally, we also performed an experiment with a substantially different calving law that does not include threshold. Alley et al.[28] suggested a set of equations for calving based on rates measured under several Antarctic ice shelves. Adapting their best law to our conceptual model results in:

$$Calv(t) = k_4 S(t) H_2(t)$$

where S represents the ice velocities at the grounding line. In our model, this velocity is strongly linked to the buttressing effect. Therefore, high values of S correspond to low buttressing which leads in the real world to high along shelf spreading. The k_4 parameter has been calibrated so as to fit the amplitude of the resulting major calving episodes to those of the standard simulation.

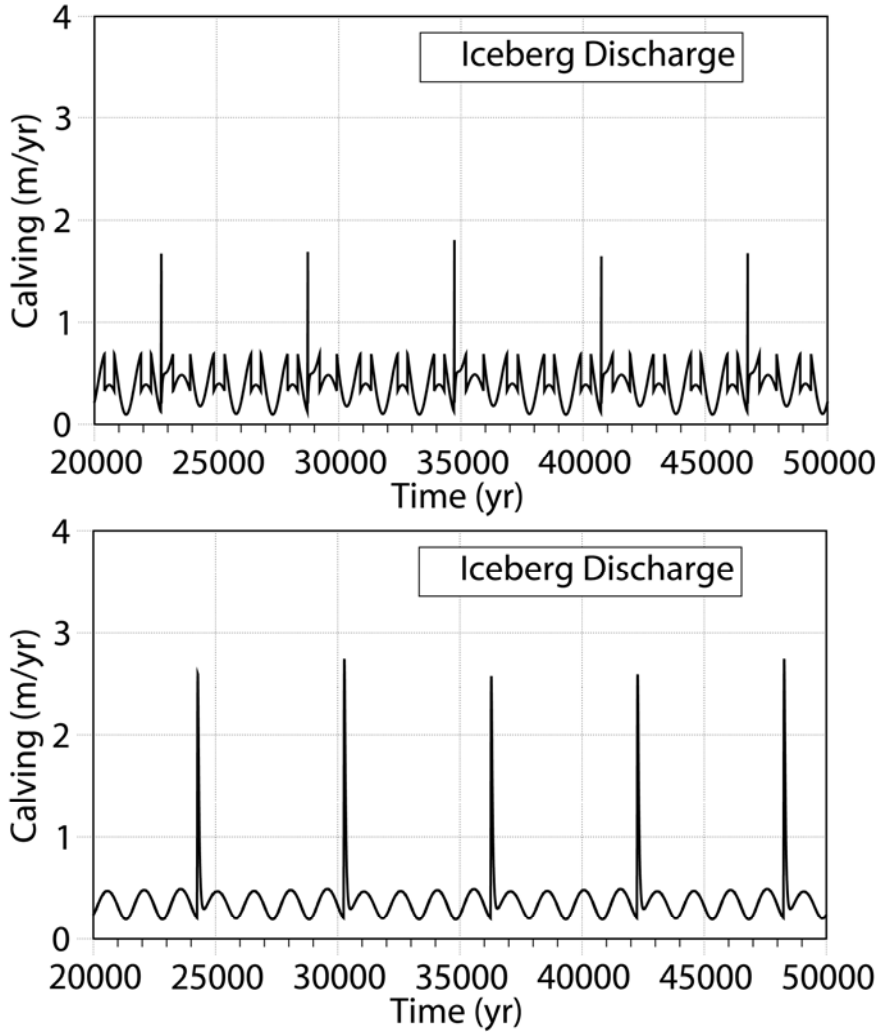

Figure S6. Sensitivity test to different calving laws.

Temporal evolution of the calving rate under a threshold-based calving law (top panel) and under an Alley-like calving law (bottom panel).

DOI: 10.1038/NGEO752

This "Alley-like" calving law produces in our model iceberg discharges compatible with our standard simulated HEs. Not considering a threshold in the calving law is not critical for the model behavior and ice flow oscillations are still present. The calving rate range in this latter case is subjected to the same condition than in our standard simulation.

SOM #7: Conclusions and outlooks

These numerous sensitivity experiments clearly show that our ice flux oscillations do not occur for a reduced combination of parameters chosen to that end, but arise for a large area of the phase space of any given parameter. This aspect further contributes to reinforce the robustness of our model and makes clearly plausible the HEs mechanism proposed in this paper.

Since our conceptual model is only devoted to discuss the mechanism under which ice flux oscillations compatible with Heinrich events occur, this paper does not deal with other important issues related to HEs. The huge atmospheric warming recorded in Greenland after HEs has been linked to a reorganization of the meridional ocean circulation (and to specific patterns of deep water formation in the North Atlantic) determining strong displacements of the sea-ice edge[36,37]. Actually, it has been proposed that for millennial-scale glacial variability the sea-ice system could play a major role[38] via a sea-ice / land-ice hysteresis phenomenon. On the other hand the explicit mechanism that allows the preservation of icebergs and IRD until the Portugal coast also remains to be largely discussed.

SOM references

5 Calov, R., Ganopolski, A., Petoukhov, V., Claussen, M., & Greve, R. Large-scale instabilities of the Laurentide ice sheet simulated in a fully coupled climate-system model. *Geophysical Research Letters* **29**, 2216-2219 (2002).

7 Rignot, E. *et al.* Accelerated ice discharge from the Antarctic Peninsula following the collapse of Larsen B ice shelf. *Geophys. Res. Lett* **31**, 18 (2004).

22 Ganopolski, A. & Rahmstorf, S. Abrupt glacial climate changes due to stochastic resonance. *Physical Review Letters* **88**, (2002).

28 Alley, R. *et al.* A Simple Law for Ice-Shelf Calving. *Science* **322**, 1344 (2008).

31 Ritz, C., Rommelaere, V., & Dumas, C. Modeling the Antarctic ice sheet evolution of the last 420 000 years: implication for altitude changes in the Vostok region. *Journal of Geophysical Research* **106**, 943-931 (2001).

32 Jenkins, A., Corr, H., Nicholls, K., Doake, C., & Stewart, C. Measuring the basal melt rate of Antarctic ice shelves using GPS and phase-sensitive radar observations. *FRISP Report* **14**, 1–8 (2003).

33 Paillard, D. & Labeyrie, L. Role of the thermohaline circulation in the abrupt warming after Heinrich events. *Nature* **372**, 162-164 (1994).

34 Levine, R. & Bigg, G.. Sensitivity of the glacial ocean to Heinrich events from different iceberg sources, as modeled by a coupled atmosphere-iceberg-ocean model. *Paleoceanography* **23** (2008).

35 Roche, D., Paillard, D., & Cortijo, E. Constraints on the duration and freshwater release of Heinrich event 4 through isotope modelling. *Nature* **432**, 379-382 (2004).

36 Li, C., Battisti, D., Schrag, D. & Tziperman, E. Abrupt climate shifts in Greenland due to displacements of the sea ice edge. *Geophys. Res. Lett* **32**, 19 (2005)).

37 Dokken, T. & Jansen, E. Rapid changes in the mechanism of ocean convection during the last glacial period. *Nature* **401**, 458-461 (1999).

38 Kaspi, Y., Sayag, R. & Tziperman, E. A ‘‘triple sea-ice state’’mechanism for the abrupt warming and synchronous ice sheet collapses during Heinrich events. *Paleoceanography* **19**(2004).

39 Sayag, R., Tziperman, E. & Ghil, M. Rapid switch-like sea ice growth and land ice-sea ice hysteresis. *Paleoceanography* **19**(2004).